Comparative Surface Studies of High-Zn-level and Commercial $Cu/ZnO/Al_2O_3$ Catalysts

H. Y. Chen, L. Chen, J. Lin,* and K. L. Tan

Surface Science Laboratory, Department of Physics, National University of Singapore, Singapore 119260

J. Li

Department of Chemistry Xiamen University, Xiamen, People's Republic of China 361005

Received: September 25, 1997; In Final Form: January 1, 1998

By altering component formulation and modifying a conventional coprecipitation procedure, we have synthesized a high-Zn-, low-Cu-level $Cu/ZnO/Al_2O_3$ catalyst which showed a 54.4 mmol/(mL catalyst h) of methanol yield and 66% CO conversion measured at 230 °C, 8 MPa, and 10000 h^{-1}. Comparative surface studies of this catalyst and the catalyst prepared according to the commercial standard (low-Zn-, high-Cu-level) were performed using microreactor study, gas (N_2 and N_2O) adsorption and X-ray photoelectron and Fourier transfer infrared spectroscopies and temperature-programmed desorption. It was found that the high-Zn-level catalyst had better performance, including a substantial (15−25%) increase in methanol yield and some other advantages under identical conditions imitating industrial process. The high catalytic activity is ascribed to the high concentrations of Cu, Zn, and oxygen vacancies detected on the surface of the high-Zn catalyst. It is proposed that the active center is Cu□ZnO and that the catalytic process may follow a carbonate−formate−methoxy−methanol mechanism. The high Zn level of the catalyst facilitates the hydrogen heterolysis with the presence of Cu, resulting in the high concentration of oxygen vacancies, as well as the existence of more Cu^{1+} ions on the surface, and thus leading to the increased CO/CO_2 adsorption, activation, and conversion.

1. Introduction

$Cu/ZnO/Al_2O_3$ (Cu/Zn/Al) catalyst has been used as industrial catalyst for methanol synthesis since 1966. Much effort has still been made in developing more effective Cu/Zn/Al catalysts by incorporating one or more promoters, modifying catalyst formulation, and improving preparation procedure.[1−6]

Recently, a high-Zn-, low-Cu-level Cu/Zn/Al catalyst has been prepared in our laboratory through altering the formulation of commercial catalyst and modifying its coprecipitation procedure. In both laboratory and pilot scale this modified catalyst has shown a better performance, including higher catalytic activity and selectivity, than that of commercial standards under identical conditions imitating the industrial process. In this paper, we report comparative studies on the modified Cu/Zn/Al and commercial catalysts at as-prepared, reduced, and reacted states using high-pressure microreactor study, gas (N_2 and N_2O) adsorption, X-ray photoelectron spectroscopy (XPS), Fourier transform infrared spectroscopy (FTIR), and temperature-programmed desorption (TPD). On the basis of these studies, the better performance of the modified catalyst is ascribed to the higher concentrations of surface Cu, Zn, and oxygen vacancies. The nature of the active sites and the mechanism of the methanol synthesis over Cu/Zn/Al catalysts are also discussed.

2. Experimental Section

2.1. Preparation of Cu/Zn/Al Catalysts. Two kinds of Cu/Zn/Al catalysts, conventional and modified, were prepared by the coprecipitation method, in which an aqueous Na_2CO_3 solution was mixed with an aqueous solution of mixed nitrates of catalyst components at a constant pH of 7−8. All chemicals used were of research grade from MERCK. The preparation of the conventional Cu/Zn/Al catalyst (Cat 1) followed the procedure reported for commercial catalysts,[7] whereas the modified Cu/Zn/Al catalyst (Cat 2) which adopted a higher ratio of the ZnO component was prepared in a slightly different manner. For the high-Zn catalyst, 1 M Na_2CO_3 solution and mixed Cu, Zn, and Al nitrate solution were both dropwisely added to deionized water. The rate of titration was carefully adjusted to be below 2 mL/min, particularly in the initial stage. The temperature of the reaction solution was maintained at 60−80 °C and its pH value kept at 7−8. Continuous stirring of the resultant solution with the precipitates was conducted for 3 h after the titration had been finished. The precipitates were aged at 80−100 °C for another 1 h, cooled to room temperature, washed three times by deionized water, dried at 110 °C for 40 h, and then calcined at 380 °C under an air stream for 24 h. The catalyst powder was made into granules with 25−35 mesh sizes. The final composition of the catalyst, as determined by inductively coupled plasma−atomic emission spectroscopy (ICP-AES), was 60:30:10 of Cu/Zn/Al weight ratio for Cat 1 and 30:60:10 for Cat 2 with no impurity elements in the catalysts.

2.2. Microreactor Study for Methanol Synthesis. A schematic of the high-pressure microreactor system is shown in Figure 1. Two vertical stainless steel reactors in the system allowed the comparative study for the two kinds of Cu/Zn/Al catalysts under identical conditions to be performed. One milliliter of 25−35 meshed catalyst was loaded into the reactor and pretreated by pure hydrogen for 24 h at 230 °C, 2.1 MPa, and 30 mL/min of flow rate. The syngas, a gas mixture of 10%

* Corresponding author. Tel, +65 8742616; e-mail, phylinjy@leonis.nus.sg.

S1089-5647(97)03112-X CCC: $15.00
Published on Web 02/24/1998

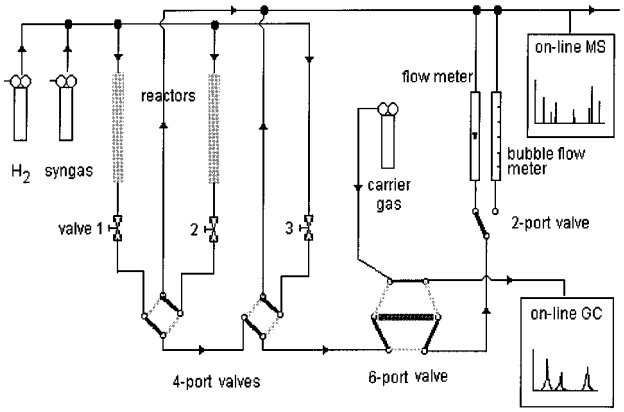

Figure 1. Schematic of microreactor setup for the evaluation of catalytic activity.

carbon monoxide, 10% carbon dioxide, and 80% hydrogen, was then fed into the system under the same conditions. The outlet gas was analyzed by on-line gas chromatography (GC) and mass spectrometry (MS Balzers QMG 064).

2.3. XPS, FTIR, and TPD Experiments. XPS measurements were conducted in a VG ESCALAB MkII, using Mg Kα source (energy 1253.6 eV) and a constant analyzer pass energy of 20 eV. With the aid of a computer program, peak fitting was executed by fixing peak width and binding energy (BE), but peak height was varied until the best fit was reached. To compensate for the charging effect, all the spectra were referenced to C1s located at 284.8 eV BE. Using a plastic glovebag, the sample transfer from the reactor to the spectrometer was made without exposing to air in order to prevent oxidation of the samples during the transportation.

Infrared spectra were recorded by a Perkin-Elmer System 2000 FTIR spectrometer equipped with a diffuse reflectance accessory and a reaction cell made by Harrick Scientific Corporation. The IR-transparent windows of the reaction cell are made of KBr. A resolution of 2 cm^{-1} was used throughout the investigation, and 64 scans taken over a 50-s interval were averaged to achieve a satisfactory signal-to-noise ratio.

TPD experiments were performed with a model AMI-M of Altamira Instruments. Prior to the experiments, the samples were pretreated by H_2 reduction at 110 °C for 1 h and 230 °C for 6 h. After a 10-min purging, the samples were further subjected to the absorbate (H_2, CO, or CO_2) exposure at room temperature for 2 h. He gas was used as the purge gas in all procedures. The flow rates of reactants and He carrier gas were both 30 mL/min. The rate of the temperature increase was 5 °C/min.

3. Results and Discussion

3.1. Microreactor Study. The methanol yields, in terms of g/mL catalyst h, obtained from the two catalysts, Cat 1 and Cat 2, under various synthesis conditions are displayed and compared in Figure 2. In general, 30−50% CO conversions were obtained under the conditions imitating the industrial process (i.e., at low temperature (around 230 °C), high pressure (2.1 MPa), and high space velocity (3600−12000 h^{-1})). At 245 °C, 8.0 MPa, and 10000 h^{-1}, 54.4 mmol/(ml catalyst h) methanol yield and 66% CO conversion have been measured on Cat 2.

Figure 2a gives the methanol yield measured at various reaction temperatures between 200 and 270 °C, while the pressure in the system is kept at 2.1 MPa and the space velocity at 3600 h^{-1}. The improved catalyst, Cat 2, shows 15−25%

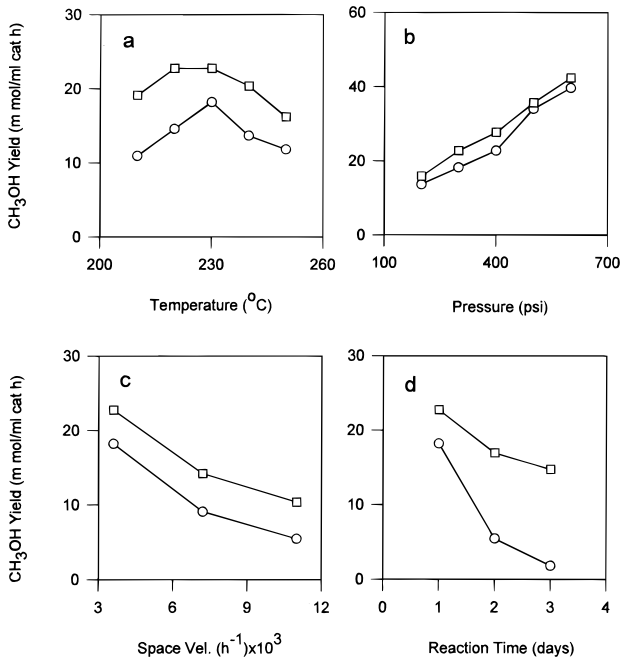

Figure 2. CH_3OH yields (mmol/ml catalyst h) vs (a) temperature, (b) pressure, (c) space velocity, and (d) reaction time. ○ for Cat 1 and □ for Cat 2.

higher methanol yield than Cat 1, although they have nearly the same surface specific area about 110 m^2/g (see section 3.2), implying higher active site concentration or higher turnover frequency of each active site for Cat 2. In Figures 2b,c, their methanol yields are plotted respectively at different values of gas pressure and space velocity, while other parameters are being kept constant. Under these conditions Cat 2 also shows a consistently better performance than Cat 1.

In Figure 2d the reduction in the CH_3OH yield after various lengths of reaction time is compared for Cat 1 and Cat 2. Although the CH_3OH yield is observed to decrease over both Cat 1 and Cat 2, after relatively long reaction time the methanol yield of Cat 2 is always higher than that of Cat 1.

3.2. Surface Specific Area and Copper Concentration. The surface areas of the Cu/Zn/Al catalysts were measured by using BET N_2 physisorption as described in the literature.[8] Almost the same values, 111 and 117 m^2/g, respectively, were obtained for Cat 1 and Cat 2 catalysts. The concentrations of metallic Cu on the catalyst surfaces after the H_2 reduction were determined by N_2O titration, being 1.77×10^{20} and 2.35×10^{20} Cu atoms/g for Cat 1 and Cat 2, respectively.

It is important that Cat 2 has higher metallic Cu concentration than Cat 1. Nevertheless it should be also noted that the higher Cu concentration obtained by this method may result from the adsorption of H_2 on ZnO during the H_2 reduction prior to the N_2O titration. Cat 2 is of high Zn level and may adsorb more H_2 (see section 3.3.2) which reacts with N_2O during titration, leading to larger consumption of N_2O.

3.3. XPS Measurements. *3.3.1. O 1s Core-Level Study.* The O 1s core-level spectra taken from as-prepared catalysts (the Cu/Zn/Al catalysts before reduction), reduced catalysts (the catalysts after reduction by H_2 under 230 °C, 2.1 MPa, and flow rate of 30 mL/min), and reacted catalysts (the catalysts after reaction under 230 °C, 2.1 MPa, and flow rate of 30 mL/min) are shown in Figure 3. For the as-prepared catalysts, the O 1s core-level peaks of Cat 1 (Figure 3a) of Cat 2 (Figure 3b) are both considerably broadened. They can be resolved, by a computer peak-fitting procedure, into three components at BEs

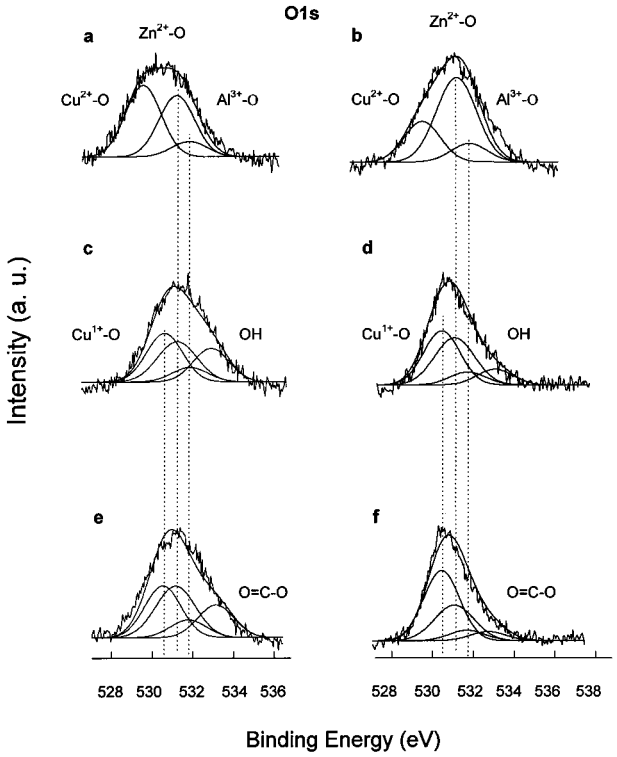

Figure 3. O 1s core-level XPS spectra: (a), (c) and (e) are taken from Cat1 and (b), (d), and (f) from Cat 2 in as-prepared, reduced, and reacted stages, respectively.

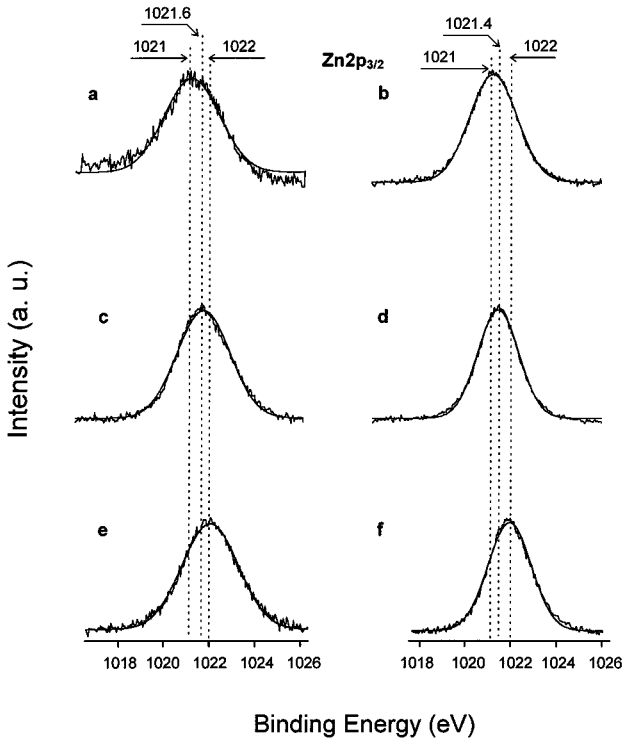

Figure 4. Zn $2p_{3/2}$ core-level XPS spectra: (a), (c), and (e) are taken from Cat 1 and (b), (d), and (f) from Cat 2 in as-prepared, reduced, and reacted stages, respectively.

529.6, 531.2, and 531.8 eV, which are assigned to the contributions of oxygen in the CuO, ZnO, and Al_2O_3 phase respectively according to references.[9,10] More oxygen component presented in CuO than that in ZnO is observed for Cat 1; whereas the case is reversed for Cat 2. This tendency is in agreement with the ICP-AES results.

After reduction by H_2, the O 1s peaks of both reduced Cat 1 and Cat 2 become sharper, with a great decrease in intensity at lower BE. The O 1s component peak at 529.6 eV is shifted to 530.6 eV, (see Figure 3c,d) which is the contribution of the oxygen in the Cu_2O phase. On the other hand, the intensity at higher BE is enhanced. The new component at 532.4 eV may be assigned to the OH group contribution,[11] resulting from the H_2 reduction.

For the O 1s core-level spectra taken from the reacted catalysts Figure 3e,f change significantly as compared to those of as-prepared catalysts. Four component peaks for the oxygen atoms bonded to Cu(I), Zn(II), Al(III), and C (BE 532.8 eV) are resolved, respectively. Note that for Cat 2 the intensity of the oxygen component presented in Cu_2O peak in the as-prepared state is low in comparison with that of the oxygen component presented in ZnO peak. It grows continually after the reduction and reaction, indicating surface $O-(Cu^{1+})$ enrichment under the reduction and reaction conditions. The O 1s peak at BE 532.8 eV is related to the oxygen atoms bonded to the carbon atoms in reaction intermediates such as formate. The oxygen atoms bonded to Al atoms remain unchanged, showing little chemical shift in all cases.

As summarized in Table 1, the relative oxygen concentration on the improved Cat 2 catalyst is always lower than that on Cat 1 no matter whether it is in as-prepared, reduced, or reacted form. The lower oxygen concentration is indicative of the loss of the oxide oxygen under reduction or reaction conditions. The more pronounced reduction in the oxygen concentration is observable in reduced and reacted Cat 2 samples, than in as-prepared catalysts. This may imply more lattice oxygen vacancies are available in this catalyst than in Cat 1. It may be worth mentioning that most of the oxygen vacancies seem to link to Zn sites as indicated by the strong decay in the oxygen component in ZnO shown in Figure 3b,d,f.

TABLE 1: Surface Relative Atomic Concentrations of Cu, Zn, O, and Al on the Catalysts, as Derived from X-ray Photoelectron Spectroscopy Data

	as-prepared catalysts		reduced catalysts		reacted catalysts	
elements detected	Cat 1 (%)	Cat 2 (%)	Cat 1 (%)	Cat 2 (%)	Cat 1 (%)	Cat 2 (%)
Al	4.5	2.9	4.4	2.7	4.5	3.1
Cu	24.0	20.3	26.4	23.0	28.8	21.4
Zn	35.5	58.5	49.0	58.7	49.7	59.7
O	36.0	18.0	20.2	15.6	17.0	15.8

The above result is also supported by thermogravimetry analysis (TG) and temperature-programmed reduction (TPR) experiments in H_2, which show greater weight loss (TG) during H_2 reduction as well as greater H_2 consumption (TPR) for Cat 2 than for Cat 1, as presented in the appendix.

3.3.2. Zn 2p Core-Level Study. Figure 4 shows the Zn $2p_{3/2}$ core-level spectra obtained from the catalyst samples at different states. In the as-prepared state both Cat 1 and Cat 2 have their Zn $2p_{3/2}$ core-level peak located at BE 1021 eV (Figure 4a,b), indicating that Zn atoms exist as ZnO.[12,13] This assignment is also supported by our Zn Auger peak measurements. After the samples were reduced in H_2, their Zn $2p_{3/2}$ peaks shift toward higher BEs at 1021.6 and 1021.4 eV for reduced Cat 1 and Cat 2, respectively (Figure 4c,d). This positive chemical shift is a result of the H_2 adsorption and heterolysis on ZnO. According to the reference,[14] H_2 can be adsorbed by ZnO in the presence of Cu in reduced Cu/ZnO catalyst and can give rise to heterolysis according to the following expression:

$$H-H + ZnO \rightarrow H^{\delta-}\ Zn-OH^{\delta+}{}_{(ad)}$$

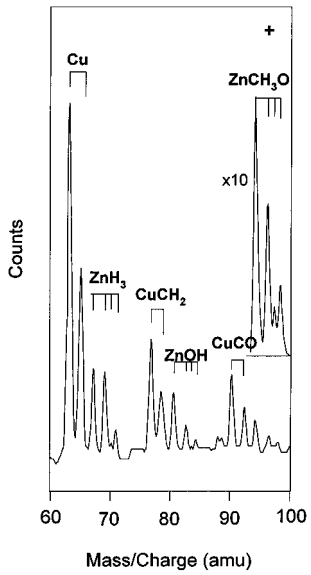

Figure 5. Positive SIMS spectrum of Cu/ZnO surface exposed to H+CO at room temperature.

In this way, $H^{\delta-}$, the adsorbed hydrogen species at the Zn site, may cause Zn 2p core-level peak to shift toward higher BE position.

We have also performed a secondary ion mass spectrometry (SIMS) study on a model Cu/ZnO catalyst, in which Cu thin film was supported on ZnO, prepared by radio-frequency-plasma-sputtered growth technique. In this experiment, hydrogen is found to be mainly held at Zn sites as evidenced by the detection of ZnH_3+ (67, 69, 70, and 71 amu) and $ZnOH^+$ (81, 83, 84, and 85 amu), as displayed in Figure 5. This supports the above conclusion that H_2 is held by heterolysis at zinc sites, thus causing a positive chemical shift of the Zn 2p core-level peak.

It is also shown in Figure 4 that after the reaction with syngas the Zn $2p_{3/2}$ core-level peak does not evidently change its overall peak shape. But further small positive chemical shifts are observable in both Figure 4e and f, being 0.4 eV for Cat 1 and 0.6 eV for Cat 2 catalysts, as compared to those of the reduced states. The shift of the Zn $2p_{3/2}$ BE up to 0.6 eV may be due to the partial oxidation of Zn atoms through the coordination of some carbon-containing intermediates, which are adsorbed at and fill the oxygen vacancies adjacent to Zn sites.

3.3.3. Cu 2p Core-Level Study. Cu2p core-level spectra are displayed in Figure 6, where it is evident that copper ions have been reduced to lower oxidation valence (Cu^0 or Cu^{1+}) after the catalysts were reduced in H_2 or reacted with the syngas.

For as-prepared catalysts, the $Cu2p_{3/2}$ core-level peak shown in Figure 6a,b is located at BE of 933.7 eV with a strong shake-up peak at 942.6 eV. It is clear that Cu atoms in as-prepared catalysts are in the Cu^{2+} state, according to the standard XPS data[10] for CuO.

The Cu $2p_{3/2}$ peak shifts to a lower BE at 932.2 eV after the catalysts were reduced in H_2. This lower binding energy peak is attributed to Cu^{1+} and Cu^0, with corresponding Cu LMM peaks at 916.8 and 918.8 eV kinetic energy, respectively[10] (Figures 7c,d). For Cat 1 the intensity ratio of Cu^0 Auger peak to Cu^{1+} Auger peak is less than 1 in the reduced state but increases to larger than 1 after the catalyst has reacted with syngas (i.e., in the reacted state). Contrarily, the ratio for Cat 2 always keeps near to 1. Copper is normally thought to be an active component for CO/CO_2 adsorption and activation. The ratio of Cu^0/Cu^{1+} would be an important parameter affecting

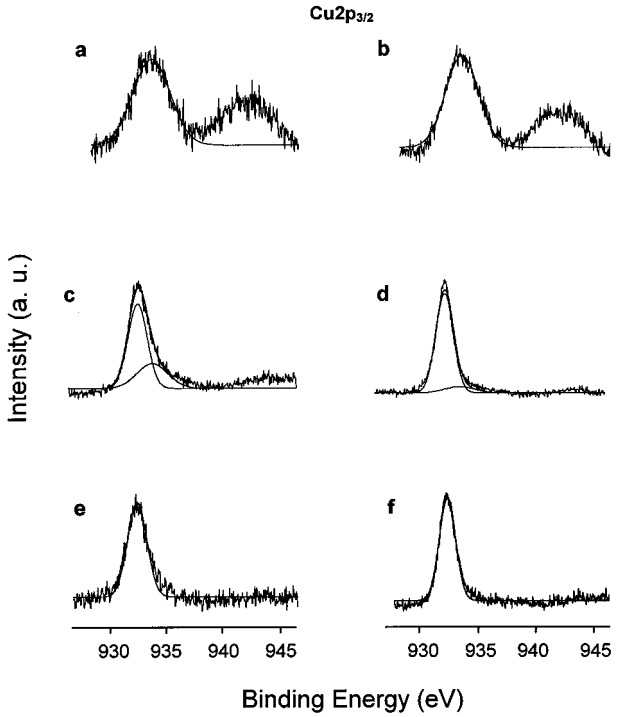

Figure 6. $Cu2p_{3/2}$ core-level XPS spectra: (a), (c), and (e) are taken from Cat 1 and (b), (d), and (f) from Cat 2 in as-prepared, reduced, and reacted stages, respectively.

the catalyst activity and selectivity. The Cu^0/Cu^{1+} couple mechanism is suggested by Bart et al. and Fujitani et al.[15,16] in which both Cu^0 and Cu^{1+} are responsible to CO and CO_2 activation. Therefore, the Cu^0/Cu^{1+} ratio in Cat 2 being around 1 is good for higher methanol yield from our experimental observation. Higher Zn component may possibly maintain high Cu^{1+} concentration by the formation of Cu^{1+}−ZnO solid solution during the reduction and reaction.

It is also noted that under identical conditions Cat 2 can be reduced to a greater extent than Cat 1 so that little Cu^{2+} is observed in Figure 6d, whereas some Cu^{2+} remained in Figure 6c for Cat 1.

3.4. FTIR Study. Figure 8 shows the IR spectra obtained from the reacted catalysts using diffuse reflectance infrared Fourier transform (DRIFT) technique. The spectra of Cat 1 (Figure 8a) and Cat 2 (Figure 8b) are basically the same. Vibrational absorbance bands are observed at 2920, 2850, 2360, 1588, 1472, 1462, 1375, and 1060−1020 cm^{-1} in the region between 1000 and 3500 cm^{-1}. The absorbance bands at 2920 and 2850 cm^{-1} are assigned to adsorbed methoxy species,[17,18] attributable to the asymmetric and symmetric ν_{C-H} vibrations, respectively. The 1588 and 1375 cm^{-1} bands with fairly strong intensity are at the positions reported for the formate adsorbed on ZnO.[19] A sharp absorbance at 1462−1472 cm^{-1} is assigned to the CO_3^{2-} carbonate symmetrical stretching vibration on ZnO according to the references.[20,21] The bands located around 2360 cm^{-1} may be due to the adsorbed CO_2 species. The band at 1060−1020 cm^{-1} is the contribution of adsorbed CH_3OH.[22]

The above IR results show that $HCOO^-$ and CO_3^{2-} species are attached to zinc sites. It is zinc formate, as well as adsorbed CO_2, which is evidently observable but not copper formate and adsorbed CO. The IR signals of copper formate are reported to be at 1600−1604 cm^{-1} [19] while the adsorbed CO at 2000−2180 cm^{-1}. It may be suggested that CO is adsorbed first at copper sites and then migrate to zinc sites. This mechanism of the Cu−Zn synergism is similar to that mentioned in the

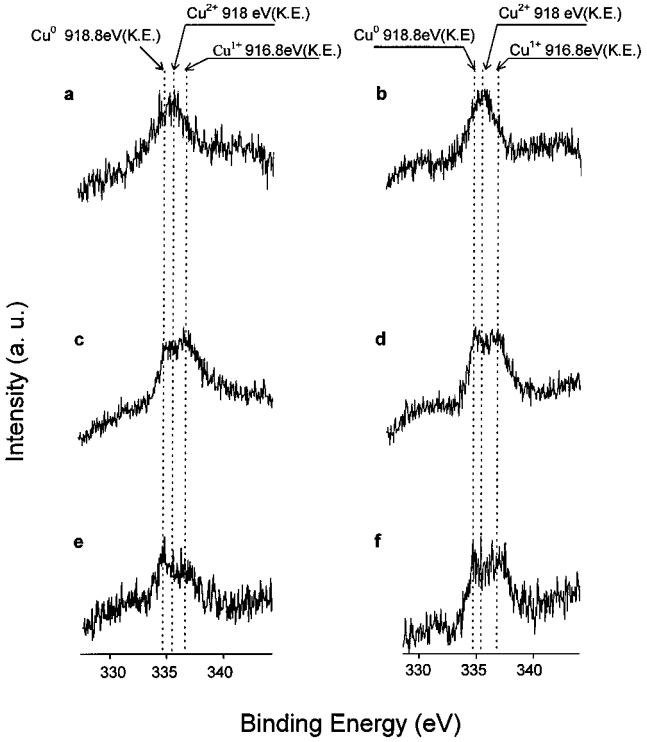

Figure 7. X-ray induced Auger Cu LMM spectra: (a), (c), and (e) are taken from Cat 1 and (b), (d), and (f) from Cat 2 in as-prepared, reduced, and reacted stages, respectively.

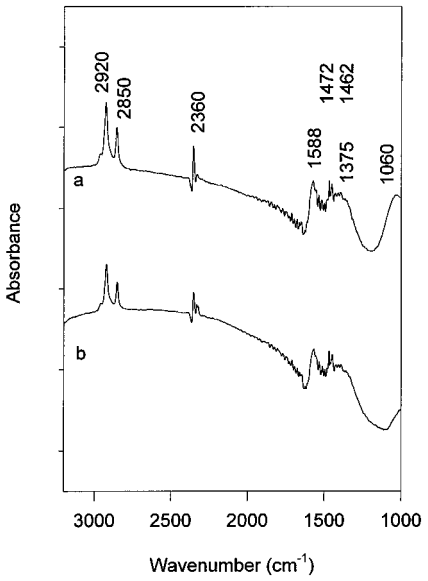

Figure 8. IR spectra (1000−3000 cm^{-1}) taken from reacted catalysts: (a) Cat 1 and (b) Cat 2.

literature,[23] and is actually reflected in our SIMS study mentioned in section 3.3.2 also. As shown in Figure 5, H is bonded to Zn sites and CO is attached to Cu (CuCO at 91, 93 amu), whereas CH_3O is detected at Zn site ($ZnCH_3O$ at 95, 97, 98, 99 amu), rather than at Cu site. This is agreeable with that reported in the literature,[24] in which the study of Cu and Zn formates confirms that methoxy zinc salt is the key intermediate for methanol formation (here note the $ZnCH_3O$ peak in our SIMS spectrum in Figure 5).

Figure 9 displays the IR absorbance between 800 and 400 cm^{-1}. There are three main absorbance bands located at 480−500, 630, and 685 cm^{-1}, which are assigned to the $Zn^{2+}-O$, $Cu^{1+}-O$ and $Al^{3+}-O$ stretching vibrations, respectively, based

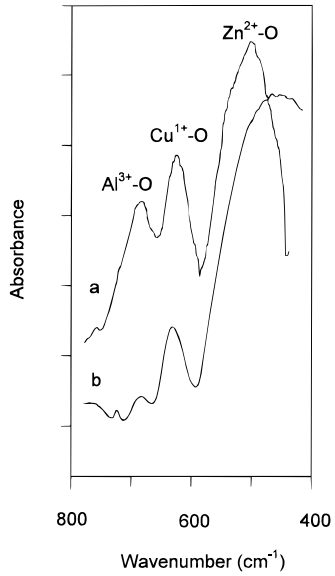

Figure 9. IR spectra (400−800 cm^{-1}) obtained from reacted samples: (a) Cat 1 and (b) Cat 2.

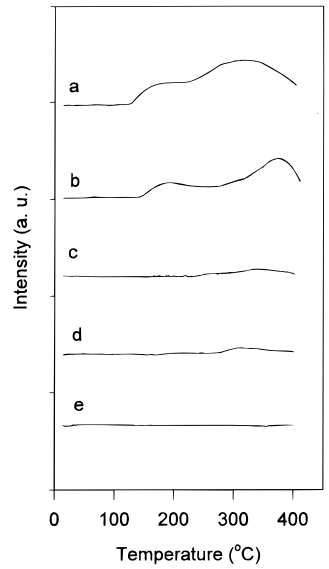

Figure 10. H_2 TPD profiles on different samples: (a) Cat 1, (b) Cat 2, (c) pure ZnO; (d) pure CuO, (e) pure Cu_2O. The He flow rate is 50 mL/min and the heating rate is 5 °C/min.

on the data obtained by us from pure ZnO, Cu_2O, and Al_2O_3, as well as from the literature.[25] The vibration of $Zn^{2+}-O$ has the strongest intensity. Its wavenumber is shifted from 510 cm^{-1} for Cat 1 to 490 cm^{-1} for Cat 2 (Figure 9b), indicating weaker Zn−O bonding strength. The weaker Zn−O bonding in Cat 2 may result in easier removal of lattice oxygen ions neighboring to Zn ions, which is in agreement with what has been observed from the XPS study (see section 3.2.2) and may be one of the important factors for higher methanol yield on Cat 2.

3.5. TPD Study: H_2 Temperature-Programmed Desorption. Figure 10 displays H_2 TPD profiles for (a) Cat 1, (b) Cat 2, (c) pure ZnO, (d) CuO, and (e) Cu_2O. Prior to the temperature-programmed desorption, the samples were first reduced by H_2 at 230 °C for 6 h and then exposed to H_2 for adsorption at room temperature as described in section 2.3. When the H_2-saturated sample is heated, the desorbed H_2 is detected as a peak at certain temperatures. In Figure 10a, for the reduced Cat 1, there is a broad peak in a wide temperature

region starting from 140 °C, with a maximum at 350 °C. For the reduced Cat 2 sample, Figure 10b shows a similar H_2 desorption profile. But the maximum desorption temperature shifts from 350 to 400 °C. The higher H_2 desorption temperature observed in Figure 10b may reflect the stronger H_2 adsorption of Cat 2. Figure 10c, d, and e are the TPD profiles obtained from pure ZnO, CuO, and Cu_2O, subjected to identical H_2 pretreatment. There is no evident H_2 desorption peak, indicating that the H_2 adsorption is rather weak on pure oxides. These results appear to indicate that hydrogen adsorption occurs only on reduced catalysts and it requires obviously the synergism of Cu and ZnO sites.

Similarly CO and CO_2 TPD profiles show higher level of CO/CO_2 adsorption for Cat 2 than Cat 1. As suggested by Frost,[26] oxygen vacancies should be considered as one kind of active sites for CO and CO_2 adsorption during methanol synthesis. Here, the important role of oxygen vacancies in the CO/CO_2 adsorption is noted, since in parallel to the higher level of CO/CO_2 adsorption we also observed higher oxygen vacancy concentration (i.e., lower surface oxygen concentration (in particular, lower level of oxygen component in ZnO)) for Cat 2 than Cat 1.

3.6. Proposed Reaction Scheme. In our study of CO hydrogenation on a $YBa_2Cu_3O_7$ thin film with well-defined Perovskite-like structure, the effect of oxygen vacancy on the CO hydrogenation to methanol is noticed, and the Cu□BaO is proposed as the active center for the CO adsorption and activation.[27] Similarly, Cu□ZnO could be postulated as the active center for the Cu/Zn/Al catalysts based on the above XPS, IR, and TPD results. It may be assumed that CO_2 or CO is first adsorbed at the Cu site, and adsorbed CO_2/CO is then bound to the adjacent Zn site (Cu−Zn synergism), forming relatively stable intermediates such as carbonate and formate, which is finally hydrogenated to methoxy and methanol. (See the following schematic reaction route.)

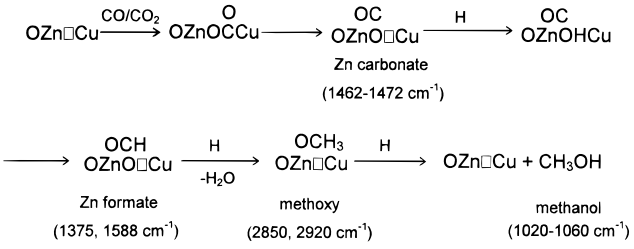

In our modified Cu/Zn/Al catalyst there is an appropriate amount of Cu which can serve as the active center for the CO and H_2 adsorption. The high level of ZnO is favorable to the hydrogen heterolysis and the formation of oxygen vacancies (through dehydration upon heating). The abundance of oxygen vacancies adjacent to Zn ions allows the Zn ions to hold more CO/CO_2 and to form relatively stable intermediates of zinc carbonate, formate, methoxy, and finally methanol. Additionally, high Zn level is also found to be in favor of the existence of Cu^{1+} on the surface, which is noted to be good for the CO/CO_2 adsorption, activation, and conversion to methanol.[28,29]

4. Summary

i. A high-Zn-level $Cu/Zn/Al_2O_3$ (Cu/Zn/Al = 30:60:10) catalyst has been prepared in our laboratory using a modified coprecipitation procedure. Under identical condition imitating industrial process (2.1 MPa and 230 °C), this catalyst has shown a better performance, including a substantial increment (15−25%) in methanol yield, as compared with the Cu/Zn/Al (60:30:10) catalyst prepared following commercial standards. Under industrial conditions, the methanol yield can reach 54.4 mmol/(mL catalyst h) with 66% CO conversion.

ii. N_2 and N_2O adsorption studies show that the high Zn catalyst has higher surface Cu concentration (2.35×10^{20} vs 1.77×10^{20} atoms/g), but about the same specific surface areas (110−120 m^2/g) as compared with the low Zn catalyst (commercial standards).

iii. XPS study shows that the high Zn catalyst has lower concentration of surface oxygen than the catalyst of commercial standard. Upon hydrogen reduction, large number of oxygen is removed from ZnO in the high Zn catalyst while the Zn 2p peak shifts to higher binding energy, probably due to hydrogen heterolysis. On the other hand, Cu^{2+} ions are reduced to Cu^0 or Cu^{1+}, and more Cu^{1+} than Cu^0 is found on the high-Zn catalyst, whereas more Cu^0 than Cu^{1+} is found on the commercial catalyst.

iv. FTIR shows lower Zn−O stretching vibration, (i.e., weaker Zn−O bonding for the high Zn catalyst as compared with that of the commercial catalyst). Carbonate, formate and methoxy groups are detected on the reacted catalysts of both high-Zn and commercial catalysts, implying a possible carbonate−formate−methoxy−methanol mechanism for the CO + CO_2 hydrogenation to methanol.

v. H_2 TPD study demonstrates that the catalyst reduction and hydrogen adsorption require the coexistence and synergism of Cu and Zn sites. The high Zn catalyst shows stronger adsorption to reactive gases, including H_2, CO, and CO_2.

vi. Cu□ZnO is considered as the active center for methanol synthesis from CO + CO_2 + H_2 over Cu/Zn/Al catalysts. The abundance of the oxygen vacancies, as well as surface Cu and Zn sites, on the high Zn catalyst, is therefore the origin of high methanol yield of the high Zn catalyst.

TABLE 2: Calibrated H_2 TG and TPR Data Obtained from Cat 1 and Cat 2 Catalysts[a]

	Cat 1	Cat 2
H_2 TG		
Y_1 (wt mg)	18.876	31.066
Y_2 (wt mg)	16.486	26.672
ΔY (wt, loss mg)	2.408	4.394
Percentage of weight loss (%)	12.75	14.14
H_2 TPR		
H_2 consumption (μL)	691.9	566.1
Sample weight (mg)	33	20
H_2 consumption per mg (μL/mg)	21	28.3

[a] Conditions: Heating rate 5 °C/min and flow rate 30 mL/min.

Appendix

In TG experiments, the catalyst was reduced by H_2, and the weight loss was recorded from Perkin-Elmer TGA 7 thermogravimetry analyzer. In TPR the 10% H_2 in Ar was introduced to react with the catalyst located in the Altamira instrument, while the temperature was increased at the rate of 5 °C/min. The H_2 consumption peak was integrated and calibrated by using built-in quantitative tube (50 μL in volume). Note that Cat 1 has a smaller percentage of weight loss as compared to Cat 2. This may mean that more oxygen is removed from Cat 2 than Cat 1 despite Cat 1 having a higher CuO level than Cat 2. TPR shows a higher H_2 consumption per milligram of Cat 2 than Cat 1. This tendency which is similar to the results derived from XPS and TG, strongly indicates that more oxygen is removed from Cat 2 than Cat 1. See Table 2.

References and Notes

(1) Saito, M.; Fujitani, T.; Takeuchi, M.; Watanabe, T. *Appl. Catal., A* **1996**, *138*, 311.

(2) Lee, J. S.; Moon, K. I.; Lee, S. H.; Lee, S. Y.; Kim, Y. G. *Catal. Lett.* **1995**, *34*, 93.
(3) Deng, J.; Sun, Q.; Zhang, Y.; Chen, S.; Wu, D. *Appl. Catal., A* **1996**, *139*, 75.
(4) Inui, T.; Takeguchi, T. *Catal. Today* **1991**, *10*, 95.
(5) Eur. Pat. 0 482 753 A2, **1991**.
(6) Chen, H. Y.; Lin, J.; Tan, K. L.; Li, J. *Appl. Surf. Sci.* In press.
(7) Fujitani, T.; Saito, M.; Kanai, Y.; Takeuchi, M.; Moriya, K.; Watanabe, T.; Kawai, M.; Kakumoto, T. *Chem. Lett.* **1993**, *6*, 1079.
(8) Karnaukhov, P.; Buyanova, N. E. In *Surface Area Determination*; Eds: Everett, D. H., Ottewill, R. H., Eds.; Butterworth: London, (**1970**).
(9) Battistoni, C.; Dormann, J. L.; Fiorani, D.; Paparazzo, E.; Viticoli, S. *Solid State Commun.* **1981**, *39*, 581.
(10) Moulder, J. F.; Stickle, W. F.; Sobol, P. E.; Bomben, K. D. *Handbook of Photoelectron Spectroscopy*; Chastain, J., Ed.; Perkin-Elmer Co. Physical Electronics Division: USA, 1992.
(11) Martensson, N.; Malmquist, P. A.; Svensson, S.; Basilier, E.; Pireaux, J. J.; Gelius, U.; Siegbahn, K. *Nouv. J. Chim.* **1977**, *1*, 191.
(12) Strohmeier, B. R.; Hercules, D. M. *J. Catal.* **1984**, *86*, 266.
(13) Nefedov, V. I.; Salyn, Y. V.; Leonhardt, G.; Scheibe, R. *J. Electron Spectrosc. Relat. Phenom.* **1977**, *10*, 121.
(14) Kokes, R. J. *Acc. Chem. Res.* **1973**, *6*, 226.
(15) Bart, J. C. J.; Sneeden, R. P. A. *Catal. Today* **1987**, *1*, 1.
(16) Fujitani, T.; Saito, M.; Kanai, Y.; Kakumoto, T.; Watanabe, T.; Nakamura, J.; Uchijima, T. *Catal. Lett.* **1994**, *25*, 271.
(17) Chinchen, G. C.; Spencer, M. S.; Waugh, K. C.; Whan, D. A. *J. Chem. Soc., Faraday Trans. 1* **1987**, *83*, 2193.
(18) Mueller, L. L.; Griffin, G. L. *J. Catal.* **1987**, *105*, 353.
(19) Neophytides, S. G.; Marchi, A. J.; Froment, G. F. *Appl. Catal.* **1992**, *A86*, 45.
(20) Millar, G. J.; Rochester, C. H.; Waugh, K. C. *J. Mol. Phys.* **1991**, *76*, 833.
(21) Little, L. H. *Infrared Spectra of Adsorbed Species*; Academic Press: New York, 1966.
(22) Bailey, S.; Froment, G. F.; Snoeck, J. W.; Waugh, K. C. *Catal. Lett.* **1995**, *30*, 99.
(23) Edwards, J. F.; Scharder, G. L. *J. Catal.* **1985**, *94*, 175.
(24) Joo, O. S.; Jung, K. D.; Han, S. H.; Uhm, S. J.; Lee, D. K.; Ihm, S. K. *Appl. Catal., A* **1996**, *135*, 273.
(25) Willis, H. A., van der Maas, J. H., Miller, R. G. J., Eds. *Laboratory Method in Vibrational Spectroscopy*; John Wiley & Sons, Ltd: New York, 1987.
(26) Frost, J. C. *Nature*, **1988**, *334*, 577.
(27) Chen, L.; Lin, J.; Chen, H. Y.; Xu, S.; Li, K.; Ong, C. K.; Tan, K. L.; Li, J. *Ber. Bunsen-Ges. Phys. Chem.* **1998**, *102*, 103.
(28) Lin, J.; Jones, P.; Guckert, J.; Solomon, E. I. *J. Am. Chem. Soc.* **1991**, *113*, 8312.
(29) Chen, H. Y.; Chen, L.; Lin, J.; Tan, K. L.; Li, J. *Inorg. Chem.* **1997**, *36*, 1417.